

Self-Learning Emulators and Eigenvector Continuation

Avik Sarkar^{1,*} and Dean Lee^{1,†}

¹*Facility for Rare Isotope Beams and Department of Physics and Astronomy,
Michigan State University, East Lansing, MI 48824, USA*

Emulators that can bypass computationally expensive scientific calculations with high accuracy and speed can enable new studies of fundamental science as well as more potential applications. In this work we focus on solving a system of constraint equations efficiently using a new machine learning approach that we call self-learning emulation. A self-learning emulator is an active learning protocol that can rapidly solve a system of equations over some range of control parameters. The key ingredient is a fast estimate of the emulator error that becomes progressively more accurate as the emulator improves. This acceleration is possible because the emulator itself is used to estimate the error, and we illustrate with two examples. The first uses cubic spline interpolation to find the roots of a polynomial with variable coefficients. The second example uses eigenvector continuation to find the eigenvectors and eigenvalues of a large Hamiltonian matrix that depends on several control parameters. We envision future applications of self-learning emulators for solving systems of algebraic equations, linear and nonlinear differential equations, and linear and nonlinear eigenvalue problems.

The frontiers of scientific discovery often reside just beyond the limits of computability. This explains the great interest across many scientific disciplines in using machine learning tools to build efficient emulators that predict scientific processes beyond what is possible with direct calculations [1–4]. However, a problem arises in that large amounts of training data for such an emulator are not possible since the required computations are difficult and expensive. In this work, we provide a potential solution to this problem when the objective is to solve a system of constraint equations over some domain of control parameters. We introduce a new machine learning method called self-learning emulation, an active learning protocol [5–7] that relies on a fast estimate of the emulator error that becomes progressively more accurate as the emulator improves. The gain in computational speed is due to the emulator itself being used to estimate the error. As we will show, self-learning emulators are highly efficient algorithms that offer both high speed and accuracy as well as a reliable estimate of the error. We will demonstrate two contrasting examples of self-learning emulators. The first example uses cubic spline interpolation to find the roots of a polynomial with variable coefficients. The second example uses eigenvector continuation to find the eigenvectors and eigenvalues of a large Hamiltonian matrix that depends on several control parameters [8, 9].

We consider a general set of simultaneous constraint equations $G_i(\mathbf{x}, \mathbf{c}) = 0$ that we solve for variables $\mathbf{x} = \{x_j\}$ as a function of control parameters $\mathbf{c} = \{c_k\}$ over some domain \mathbf{D} . Let us denote the exact solutions as $\mathbf{x}(\mathbf{c})$. We assume that we have an emulator which can take the exact solutions for some set of training points $\{\mathbf{c}^{(i)}\}$ and construct an approximate solution $\tilde{\mathbf{x}}(\mathbf{c})$ for all $\mathbf{c} \in \mathbf{D}$. Let us define the error or loss function as $\|\Delta\mathbf{x}(\mathbf{c})\|$, where $\Delta\mathbf{x}(\mathbf{c}) = \mathbf{x}(\mathbf{c}) - \tilde{\mathbf{x}}(\mathbf{c})$. The objective is to train the emulator to minimize the peak value of the error function over the domain \mathbf{D} using as few additional training points as possible.

Since the error function will vary over many orders of magnitude, it is more convenient to work with the logarithm of the error function, $\log\|\Delta\mathbf{x}(\mathbf{c})\|$. The emulator will reproduce the

exact solution at the training points $\{\mathbf{c}^{(i)}\}$. Therefore, the logarithm of error function will become a rapidly varying function of \mathbf{c} as we include more training points.

Let us consider the case where $\Delta\mathbf{x}(\mathbf{c})$ is small enough that we can accurately expand the constraint equations as $G_i(\tilde{\mathbf{x}}(\mathbf{c}), \mathbf{c}) + \Delta\mathbf{x}(\mathbf{c}) \cdot \nabla_{\tilde{\mathbf{x}}} G_i(\tilde{\mathbf{x}}(\mathbf{c}), \mathbf{c}) \approx 0$. If the number of degrees of freedom is small, we can solve the linear inversion problem for $\Delta\mathbf{x}(\mathbf{c})$ and provide a fast estimate for the logarithm of the error. This estimate is nothing more than the multivariate form of the Newton-Raphson method. Some care must be taken if the matrix inversion becomes ill-defined, and we show how this can be handled with a numerical regulator when discussing our polynomial root example later.

For most cases of interest, however, there will be many degrees of freedom and the matrix inversion required to solve for $\Delta\mathbf{x}(\mathbf{c})$ will be too slow for our self-learning emulator training process. We therefore choose another non-negative functional $F[\{G_i(\tilde{\mathbf{x}}(\mathbf{c}), \mathbf{c})\}]$ as a surrogate for $\|\Delta\mathbf{x}(\mathbf{c})\|$. The only essential requirement we impose on $F[\{G_i(\tilde{\mathbf{x}}(\mathbf{c}), \mathbf{c})\}]$ is that it is linearly proportional to $\|\Delta\mathbf{x}(\mathbf{c})\|$ in the limit $\|\Delta\mathbf{x}(\mathbf{c})\| \rightarrow 0$. Let us write the logarithm of the error as

$$\log\|\Delta\mathbf{x}(\mathbf{c})\| = \log F[\{G_i(\tilde{\mathbf{x}}(\mathbf{c}), \mathbf{c})\}] + A + B(\mathbf{c}), \quad (1)$$

where A is a constant and the average of $B(\mathbf{c})$ over the domain \mathbf{D} is zero. Since $F[\{G_i(\tilde{\mathbf{x}}(\mathbf{c}), \mathbf{c})\}]$ is linearly proportional to $\|\Delta\mathbf{x}(\mathbf{c})\|$ in the limit $\|\Delta\mathbf{x}(\mathbf{c})\| \rightarrow 0$, the function $\log F[\{G_i(\tilde{\mathbf{x}}(\mathbf{c}), \mathbf{c})\}]$ will have the same steep hills and valleys as the function $\log\|\Delta\mathbf{x}(\mathbf{c})\|$ as we include more training points. In the limit of large number of training points, we can neglect the much smaller variation of $B(\mathbf{c})$ over the domain \mathbf{D} . We can therefore approximate the logarithm of the error as $\log F[\{G_i(\tilde{\mathbf{x}}(\mathbf{c}), \mathbf{c})\}] + A$.

We now have in hand a fast estimate for the logarithm of the error that becomes progressively more accurate as more training points are added. The self-learning emulator training program is a greedy algorithm where we search to find the point \mathbf{c} where the logarithm of the error is greatest. We then add this point to the training set and repeat the whole process. We note that the unknown constant A is irrelevant for compar-

ing the logarithm of the error for different points \mathbf{c} . Nevertheless, we can also quickly estimate A simply by taking several random samples of \mathbf{c} and computing the average value of the difference between $\log\|\Delta\mathbf{x}(\mathbf{c})\|$ and $\log F[\{G_i(\tilde{\mathbf{x}}(\mathbf{c}), \mathbf{c})\}]$. In this manner we have constructed a fast emulator that becomes more and more accurate as more training points are added and provides a reliable estimate of the emulator error. We note that while the name is similar to another active learning method called self-learning Monte Carlo [10], the purpose, training, and applications of self-learning emulators are quite different.

Self-learning emulation can be used with any emulator, whether it is a straightforward technique such as polynomial interpolation or Gaussian processes, or a more involved method such as neural networks or eigenvector continuation. It can also be applied to any system of constraints such as algebraic equations, linear and nonlinear differential equations, and linear and nonlinear eigenvalue problems. The first example we present, Model 1, uses a natural cubic spline emulator to find the lowest real root of an odd-degree polynomial with real coefficients.

For Model 1 we consider an order n polynomial of the form $p(x) = c_n x^n + \dots + c_1 x + c_0$, where n is odd and the coefficients are real. Since n is odd, the polynomial crosses zero at least once if $c_n \neq 0$, and so we can uniquely define the lowest real root. We will consider the case where all of the coefficients are fixed and only the coefficient c_{n-1} is varied. Let $x(c_{n-1})$ be the exact lowest real root. We start with at least three training points for c_{n-1} and use natural cubic splines to define the cubic spline approximation $\tilde{x}(c_{n-1})$ for all values of c_{n-1} . The logarithm of the error function is then $\log|\Delta x(c_{n-1})|$ where $\Delta x(c_{n-1}) = x(c_{n-1}) - \tilde{x}(c_{n-1})$. We can estimate $|\Delta x(c_{n-1})|$ using the Newton-Raphson method,

$$|\Delta x(c_{n-1})| \approx \frac{|p(\tilde{x}(c_{n-1}))|}{\sqrt{|p'(\tilde{x}(c_{n-1}))|^2 + \epsilon^2}}, \quad (2)$$

where we have included a small regulator ϵ to avoid divergences when the derivative p' vanishes.

For our example, we take a fifth-order polynomial, $n = 5$, with coefficients $c_5 = 5, c_3 = 3, c_2 = 2, c_1 = 1, c_0 = 1$. We also set $\epsilon = 1$ as defined in Eq. (2). In Fig. 1 we show results for the estimate of the logarithm of the error starting from four training points spanning the interval from $c_4 = 0$ to $c_4 = 100$. For each iteration, the self-learning algorithm is choosing a new training point that corresponds to the location of the maximum of estimated error function from the previous iteration. In Fig. 2 we show that there is excellent agreement between the logarithm of the error for the actual error and the error estimate after 10 iterations. We note that the error has dropped significantly for all values of c_4 from the original error estimate in Fig. 1, indicating that the self-learning emulator is functioning as intended. The fact that more training points are needed for smaller values of c_4 shows that the training process is not simply adding more training points at random, but is instead uniformly improving the emulator performance across the entire domain. For Model 1, we find that the fast error estimate in our self-learning protocol provides

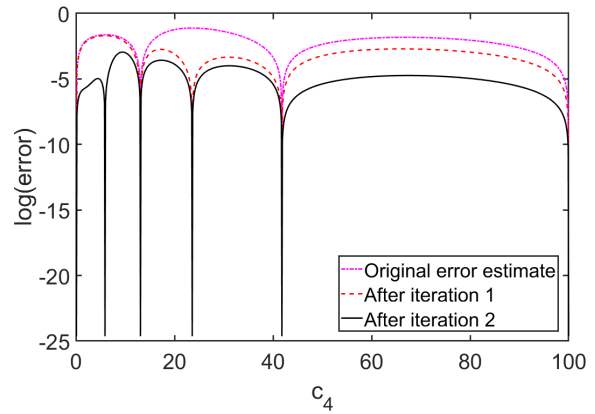


FIG. 1: Estimates of the logarithm of the error for the cubic spline self-learning emulator, which finds the lowest real root of the fifth order polynomial $p(x)$ in Model 1. We show results after iteration 0, 1, and 2.

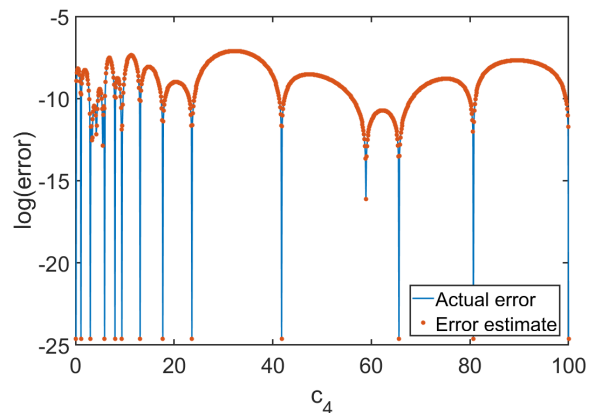


FIG. 2: Logarithm of the actual error and error estimate for the cubic spline self-learning emulator in Model 1 after 10 iterations.

a factor of 200 times greater computational speed over tuning the cubic spline emulator using direct calculations of the error.

For our next example we will use eigenvector continuation as the emulator. Eigenvector continuation (EC) is a variational method that finds the extremal eigenvalues and eigenvectors of Hamiltonian matrix that depends on one or more control parameters [11]. The method consists of projecting the Hamiltonian onto a subspace spanned by a set of training eigenvectors, which are the exact eigenvectors of the Hamiltonian at some chosen training values of the control parameters, and then solving the generalized eigenvalue problem. This projection reduces the computational complexity greatly, and EC allows one to compute the eigenvector in a region of the parameter where it was not computationally feasible to solve the eigenvalue problem directly and has been used for dealing with Monte Carlo sign oscillations [12] and as a resummation method for perturbation theory [13, 14]. Recently it was observed that EC can function as an accurate emulator

for quantum systems [8], and this was followed by a number of new developments and applications [9, 15–20]. The implementation of EC within an active learning framework was first discussed in [21]. However, one faces a computational bottleneck for large systems if the training process requires many direct calculations of eigenvectors. In this work we propose instead to use an fast estimate of the error function based upon the variance of the Hamiltonian.

Let $H(\mathbf{c})$ be a manifold of Hamiltonians where the dependence on the control parameters \mathbf{c} is smooth. Let $|v(\mathbf{c})\rangle$ be the corresponding eigenvector of interest and $E(\mathbf{c})$ be the corresponding energy eigenvalue. The EC approximation consists projecting $H(\mathbf{c})$ onto the subspace spanned by the training eigenvectors $\{|v(\mathbf{c}^{(i)})\rangle\}$. By solving the generalized eigenvalue, we obtain the EC approximation to the eigenvector $|\tilde{v}(\mathbf{c})\rangle$. Throughout our discussion, we assume that all eigenvectors are unit normalized. The corresponding approximate energy $\tilde{E}(\mathbf{c})$ is equal to the expectation value $\langle \tilde{v}(\mathbf{c}) | H(\mathbf{c}) | \tilde{v}(\mathbf{c}) \rangle$.

The logarithm of the error is $\log \|\Delta v(\mathbf{c})\|$, where $|\Delta v(\mathbf{c})\rangle = |v(\mathbf{c})\rangle - |\tilde{v}(\mathbf{c})\rangle$. Computing the error directly will be computationally too expensive for large systems, and so we will instead work with $\log F[\tilde{v}(\mathbf{c}), H(\mathbf{c})]$, where $F[\tilde{v}(\mathbf{c}), H(\mathbf{c})]$ is proportional to the square root of the variance of the Hamiltonian,

$$F[\tilde{v}(\mathbf{c}), H(\mathbf{c})] = \sqrt{\frac{\langle \tilde{v}(\mathbf{c}) | [H(\mathbf{c}) - \tilde{E}(\mathbf{c})]^2 | \tilde{v}(\mathbf{c}) \rangle}{\langle \tilde{v}(\mathbf{c}) | [H(\mathbf{c})]^2 | \tilde{v}(\mathbf{c}) \rangle}}. \quad (3)$$

We note that $F[\tilde{v}(\mathbf{c}), H(\mathbf{c})]$ will be linearly proportional to $\|\Delta v(\mathbf{c})\|$ in the limit $\|\Delta v(\mathbf{c})\| \rightarrow 0$. Therefore $\log F[\tilde{v}(\mathbf{c}), H(\mathbf{c})]$ can be used as a surrogate for the logarithm of the error.

In our next example, Model 2, we consider the ground state of a system of four distinguishable particles with equal masses on a three-dimensional lattice with zero-range interactions. We will work in lattice units where physical quantities are multiplied by the corresponding power of the lattice spacing to make dimensional combinations. Furthermore, we set the particles masses to equal 1 in lattice units. We label the particles as 1, 2, 3, 4 and take the control parameters to be the six possible pairwise interactions, c_{ij} , with $i < j$. The lattice volume is a periodic cube of size $L^3 = 4^3$, and the corresponding Hamiltonian is a linear space with 262, 144 dimensions. The details of the Hamiltonian can be found in the Supplemental Material. This model can be viewed as a generalization of the four two-component fermions with zero-range interactions considered in [18, 22] or the Bose-Hubbard model considered in [11].

We would like to study the appearance of interesting structures such as particle clustering, repulsive spatial correlations, deformations, and/or diffuse halo structures in the ground state wave function as a function of the six coupling parameters c_{ij} . Such detailed global studies are difficult due to the number of repeated calculations necessary. However, we now show that self-learning emulation with eigenvector continua-

tion can make such studies fairly straightforward.

Since it is difficult to visualize data for all six parameters, we first present results corresponding to one two-dimensional slice. We set $c_{14} = c_{23} = c_{24} = c_{34} = -2.3475$ and use EC as an emulator for the ground state as a function of c_{12} and c_{13} over a square domain where each coefficient ranges from -5 to 5 . We initialize the self-learning emulator with one random training point for c_{12} and c_{13} . When searching for new training points we use the method of simulated annealing [23] with an energy functional given by $-\log F[\tilde{v}(\mathbf{c}), H(\mathbf{c})]$.

In Fig. 3 we show the logarithm of the error obtained after 40 iterations. In (a) we show the logarithm of the actual error, and in (b) we show the logarithm of the estimated error. As predicted in Eq. (1), we see that the two plots are approximately the same up to a constant offset A , with $A \approx -2.3$. The peak value of the actual error is $\|\Delta v(\mathbf{c})\| = 2 \times 10^{-5}$. From the figure we see that the local maxima of the error reside along an approximately flat horizontal surface. The flatness of this surface indicates that our self-learning emulator is performing as intended, with the training algorithm removing the peak error at each iteration. This is a highly nontrivial result, since the actual error is never calculated in the training protocol. We note that the distribution of training points is far from uniform. The region near the line $c_{12} + c_{13} = -1$ has a higher density of training points, indicating that the ground state wave function has a more complicated dependence on c_{12} and c_{13} in that location.

Using the self-learning emulator, we can measure short-range correlations between pairs of particle in the ground state wave function for all values of c_{12} and c_{13} . In Fig. 3 we show the short-range correlations for pairs of particles 1 with 2 and 1 with 3. The correlation function ρ_{12} measures the probability that particles 1 and 2 occupy the same lattice site, and the correlation function ρ_{13} measures the probability that particles 1 and 3 occupy the same lattice site. We see that ρ_{12} is close to zero when c_{12} is positive and rises to a peak of 1 when c_{12} is negative and increasing in magnitude. Similarly, ρ_{13} is close to zero when c_{13} is positive and rises to a peak of 1 when c_{13} is negative and increasing in magnitude. An examination of the other short-range correlation functions, $\rho_{14}, \rho_{23}, \rho_{24}, \rho_{34}$, shows that for all values of c_{12} and c_{13} in our domain, the four-body system remains a compact bound state. However, when c_{12} or c_{13} are positive, we induce a repulsive spatial separation between the corresponding particles within the bound state wave function.

We now consider the case where we vary each of the six control parameters c_{ij} in Model 2 over the range from -5 to 0 . We again use simulated annealing with the energy functional $-\log F[\tilde{v}(\mathbf{c}), H(\mathbf{c})]$ to find the optimal training points. After learning the eigenvector manifold with self-learning EC, we calculate the exact error at a few random points in order determine the unknown constant A in Eq. (1) and determine the logarithm of the error. After 80 iterations, the peak value of the error is $\|\Delta v(\mathbf{c})\| = 4 \times 10^{-3}$. For this example, Model 2, the self-learning emulator provides a factor of 100 computational advantage over tuning the EC emulator using direct

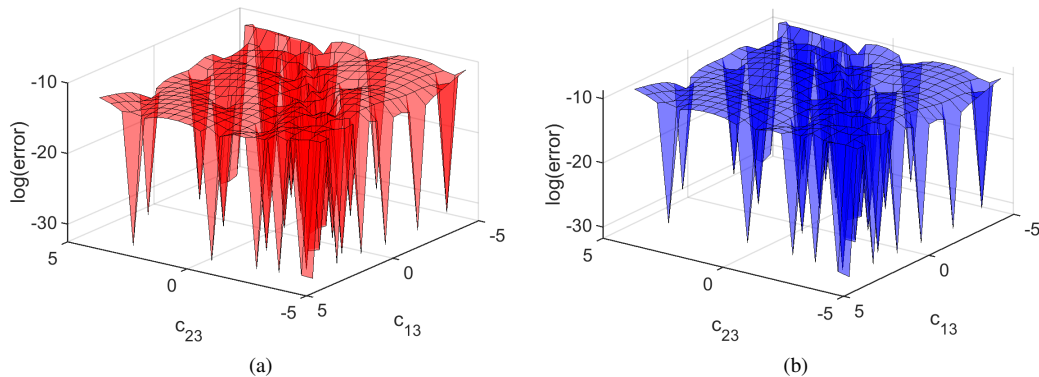


FIG. 3: Logarithm of the error in Model 2 after 40 iterations using self-learning EC. In (a) we show the logarithm of the actual error (red), and in (b) we show the logarithm of the estimated error (blue).

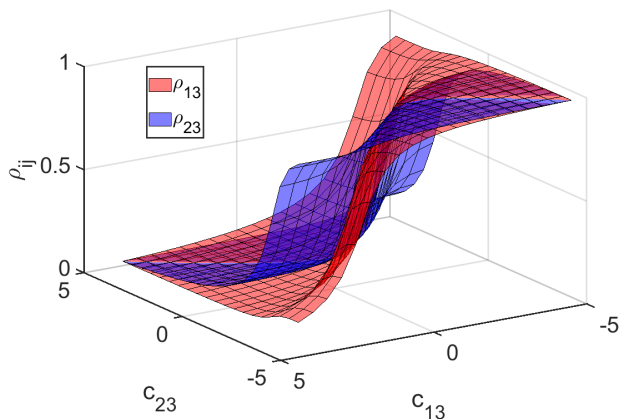


FIG. 4: Plot of the two-particle short-range correlations in Model 2. ρ_{13} (red) measures the probability that particles 1 and 3 occupy the same lattice site, and the correlation function ρ_{23} (blue) measures the probability that particles 2 and 3 occupy the same lattice site.

calculations of the error.

With these two examples, Model 1 and Model 2, we see that the computational advantages of self-learning emulators are clear. The self-learning emulator is using the emulator for the training regimen, and performing direct calculations only for the selected new training points. Hence, the computational speed that one gains in using a self-learning emulator is equal to the acceleration factor of the emulator itself, which can grow to five order of magnitudes or more for large systems [9]. Self-learning emulation can be implemented with other emulators in the future in order to efficiently solve systems of algebraic equations, linear and nonlinear differential equations, and linear and nonlinear eigenvalue problems. Some additional insights and details about self-learning eigenvector continuation are given in the Supplemental Material.

We are grateful for discussions with Joey Bonitati, Gabriel Given, Caleb Hicks, Morten Hjorth-Jensen, Daniel Lee, Witek Nazarewicz, Esmond Ng, Zhengrong Qian, James Vary, Ja-

cob Watkins, Stefan Wild, and Chao Yang. We gratefully acknowledge funding by the U.S. Department of Energy (DE-SC0013365 and DE-SC0021152) and the Nuclear Computational Low-Energy Initiative (NUCLEI) SciDAC-4 project (DE-SC0018083) as well as computational resources provided by the Oak Ridge Leadership Computing Facility through the INCITE award “Ab-initio nuclear structure and nuclear reactions”, the Gauss Centre for Supercomputing e.V. (www.gauss-centre.eu) for computing time on the GCS Supercomputer JUWELS at Jülich Supercomputing Centre (JSC), and Michigan State University.

* Electronic address: sarkarav@msu.edu

† Electronic address: leed@frib.msu.edu

- [1] G. Carleo, I. Cirac, K. Cranmer, L. Daudet, M. Schuld, N. Tishby, L. Vogt-Maranto, and L. Zdeborová, *Rev. Mod. Phys.* **91**, 045002 (2019).
- [2] J. J. Thiagarajan, B. Venkatesh, R. Anirudh, P.-T. Bremer, J. Gaffney, G. Anderson, and B. Spears, *Nature Communications* **11**, 5622 (2020), 2005.02328.
- [3] M. F. Kasim, D. Watson-Parris, L. Deaconu, S. Oliver, P. Hatfield, D. H. Froula, G. Gregori, M. Jarvis, S. Khatiwala, J. Korenaga, et al., *arXiv e-prints arXiv:2001.08055* (2020), 2001.08055.
- [4] P. Bedaque et al., *Eur. Phys. J. A* **57**, 100 (2021), 2006.05422.
- [5] B. Settles, *Computer Sciences Technical Report 1648*, University of Wisconsin–Madison (2009).
- [6] D. A. Cohn, Z. Ghahramani, and M. I. Jordan, *Journal of artificial intelligence research* **4**, 129 (1996).
- [7] D. Cohn, L. Atlas, and R. Ladner, *Machine learning* **15**, 201 (1994).
- [8] S. König, A. Ekström, K. Hebel, D. Lee, and A. Schwenk (2019), 1909.08446.
- [9] A. Ekström and G. Hagen, *Phys. Rev. Lett.* **123**, 252501 (2019), 1910.02922.
- [10] J. Liu, Y. Qi, Z. Y. Meng, and L. Fu, *Physical Review B* **95** (2017), ISSN 2469-9969.
- [11] D. Frame, R. He, I. Ipsen, D. Lee, D. Lee, and E. Rrapaj, *Phys. Rev. Lett.* **121**, 032501 (2018), 1711.07090.

- [12] D. K. Frame, Ph.D. thesis (2019), 1905.02782.
- [13] P. Demol, T. Duguet, A. Ekström, M. Frosini, K. Hebler, S. König, D. Lee, A. Schwenk, V. Somà, and A. Tichai, *Phys. Rev. C* **101**, 041302(R) (2020), 1911.12578.
- [14] P. Demol, M. Frosini, A. Tichai, V. Somà, and T. Duguet, *Annals Phys.* **424**, 168358 (2021), 2002.02724.
- [15] R. J. Furnstahl, A. J. Garcia, P. J. Millican, and X. Zhang, *Phys. Lett. B* **809**, 135719 (2020), 2007.03635.
- [16] D. Bai and Z. Ren, *Phys. Rev. C* **103**, 014612 (2021), 2101.06336.
- [17] S. Wesolowski, I. Svensson, A. Ekström, C. Forssén, R. J. Furnstahl, J. A. Melendez, and D. R. Phillips (2021), 2104.04441.
- [18] A. Sarkar and D. Lee, *Phys. Rev. Lett.* **126**, 032501 (2021).
- [19] S. Yoshida and N. Shimizu (2021), 2105.08256.
- [20] J. A. Melendez, C. Drischler, A. J. Garcia, R. J. Furnstahl, and X. Zhang (2021), 2106.15608.
- [21] C. Eklind, Ph.D. thesis (2021), <https://hdl.handle.net/20.500.12380/302455>.
- [22] S. Bour, X. Li, D. Lee, U.-G. Meißner, and L. Mitas, *Phys. Rev. A* **83**, 063619 (2011), arXiv:1104.2102 [cond-mat.quant-gas].
- [23] M. Pincus, *Operations Research* **18**, 1225 (1970).

SUPPLEMENTAL MATERIAL

Geometrical picture of eigenvector continuation error

We will present a geometrical picture of eigenvector continuation (EC) error as well as some additional insight into the error estimate that appears in Eq. (3) of the main text. We consider a Hamiltonian manifold $H(\mathbf{c})$ that depends on the control parameters \mathbf{c} . We write $|v(\mathbf{c})\rangle$ for the eigenvector of interest and $E(\mathbf{c})$ for the corresponding energy eigenvalue. Suppose we know the eigenvectors at M different training points, $\{\mathbf{c}^{(1)}, \dots, \mathbf{c}^{(M)}\}$. We label the set of M training eigenvectors as $S_M = \{|v(\mathbf{c}^{(1)})\rangle, \dots, |v(\mathbf{c}^{(M)})\rangle\}$. Let us define the norm matrix $\mathcal{N}(S_M)$ as

$$\begin{bmatrix} \langle v(\mathbf{c}^{(1)})|v(\mathbf{c}^{(1)})\rangle & \dots & \langle v(\mathbf{c}^{(1)})|v(\mathbf{c}^{(M)})\rangle \\ \vdots & \ddots & \vdots \\ \langle v(\mathbf{c}^{(M)})|v(\mathbf{c}^{(1)})\rangle & \dots & \langle v(\mathbf{c}^{(M)})|v(\mathbf{c}^{(M)})\rangle \end{bmatrix}, \quad (\text{S1})$$

and let $\Omega^2(S_M)$ be the determinant of $\mathcal{N}(S_M)$. Then $\Omega^2(S_M)$ corresponds to the square of the volume of the M -dimensional parallelepiped defined by the vectors in the set S_M . If all the eigenvectors are normalized, then the maximum possible volume is 1, which is attained when all the eigenvectors are orthogonal.

Let us now consider selecting the next training point, \mathbf{c}_{M+1} . Let P be the projection operator onto the linear span of S_M , and let Q be the orthogonal complement so that $Q = 1 - P$. Suppose we now expand our training set S_M by adding another training vector $|v(\mathbf{c})\rangle$ to form S_{M+1} . Let us define the perpendicular projection vector $|v_\perp(\mathbf{c})\rangle$ as

$$|v_\perp(\mathbf{c})\rangle = Q|v(\mathbf{c})\rangle. \quad (\text{S2})$$

Since $\Omega^2(S_M)$ is the squared volume of the parallelepiped defined by the vectors in S_M and $\Omega^2(S_{M+1})$ is the squared volume of the parallelepiped defined by the vectors in S_{M+1} , it follows that the ratio $\Omega^2(S_{M+1})$ to $\Omega^2(S_M)$ is given by the squared norm of $|v_\perp(\mathbf{c})\rangle$,

$$\frac{\Omega^2(S_{M+1})}{\Omega^2(S_M)} = \langle v_\perp(\mathbf{c})|v_\perp(\mathbf{c})\rangle. \quad (\text{S3})$$

Let us define the projections of H onto P and Q subspaces as

$$H^P(\mathbf{c}) = PH(\mathbf{c})P, \quad H^Q(\mathbf{c}) = QH(\mathbf{c})Q. \quad (\text{S4})$$

The EC approximation is nothing more than the approximation of $|v(\mathbf{c})\rangle$ by some eigenvector of $H^P(\mathbf{c})$, which we denote as $|v^P(\mathbf{c})\rangle$. Let the corresponding energy be labelled $E^P(\mathbf{c})$ so that

$$H^P(\mathbf{c})|v^P(\mathbf{c})\rangle = E^P(\mathbf{c})|v^P(\mathbf{c})\rangle. \quad (\text{S5})$$

We also label the eigenvectors of $H^Q(\mathbf{c})$ contained in the orthogonal complement Q as,

$$H^Q(\mathbf{c})|v_j^Q(\mathbf{c})\rangle = E_j^Q(\mathbf{c})|v_j^Q(\mathbf{c})\rangle. \quad (\text{S6})$$

When the difference between the exact eigenvector and the eigenvector continuation approximation of the eigenvector is small, we can use first order perturbation theory to write

$$|v(\mathbf{c})\rangle \approx |v^P(\mathbf{c})\rangle + \sum_j \frac{\langle v_j^Q(\mathbf{c})|H(\mathbf{c})|v^P(\mathbf{c})\rangle}{E^P(\mathbf{c}) - E_j^Q(\mathbf{c})} |v_j^Q(\mathbf{c})\rangle. \quad (\text{S7})$$

To first order in perturbation theory, the residual vector is just $|v_\perp(\mathbf{c})\rangle \approx |v(\mathbf{c})\rangle - |v^P(\mathbf{c})\rangle$. We therefore have

$$|v_\perp(\mathbf{c})\rangle \approx \sum_j \frac{\langle v_j^Q(\mathbf{c})|H(\mathbf{c})|v^P(\mathbf{c})\rangle}{E^P(\mathbf{c}) - E_j^Q(\mathbf{c})} |v_j^Q(\mathbf{c})\rangle \quad (\text{S8})$$

If we now combine with Eq. (S3), we get

$$\frac{\Omega^2(S_{M+1})}{\Omega^2(S_M)} = \||v_\perp(\mathbf{c})\rangle\|^2 = \sum_j \frac{\langle v^P(\mathbf{c})|H(\mathbf{c})|v_j^Q(\mathbf{c})\rangle \langle v_j^Q(\mathbf{c})|H(\mathbf{c})|v^P(\mathbf{c})\rangle}{[E^P(\mathbf{c}) - E_j^Q(\mathbf{c})]^2}. \quad (\text{S9})$$

We can now connect this result with the error or loss function in the main text. The second part of the equation gives an expression for the error term $\|v_{\perp}(\mathbf{c})\|$ using first-order perturbation theory, and the first part of the equation is a geometrical interpretation of the error term as the ratio of the squared volumes, $\Omega^2(S_{M+1})$ to $\Omega^2(S_M)$. Taking the logarithm of the square root, we get

$$\log\|v_{\perp}(\mathbf{c})\| = \frac{1}{2} \log \sum_j \frac{\langle v^P(\mathbf{c})|H(\mathbf{c})|v_j^Q(\mathbf{c})\rangle \langle v_j^Q(\mathbf{c})|H(\mathbf{c})|v^P(\mathbf{c})\rangle}{[E^P(\mathbf{c}) - E_j^Q(\mathbf{c})]^2}. \quad (\text{S10})$$

The term in the numerator,

$$\langle v^P(\mathbf{c})|H(\mathbf{c})|v_j^Q(\mathbf{c})\rangle \langle v_j^Q(\mathbf{c})|H(\mathbf{c})|v^P(\mathbf{c})\rangle, \quad (\text{S11})$$

will go to zero at each of the training points, causing large variations in the logarithm of the error as we add more and more training points. In contrast, the term in the denominator, $[E^P(\mathbf{c}) - E_j^Q(\mathbf{c})]^2$, will be smooth as a function of c . Similarly, $\langle v^P(\mathbf{c})|[H(\mathbf{c})]^2|v^P(\mathbf{c})\rangle$ will also be a smooth function of \mathbf{c} . We can write

$$\log \sum_j \frac{\langle v^P(\mathbf{c})|H(\mathbf{c})|v_j^Q(\mathbf{c})\rangle \langle v_j^Q(\mathbf{c})|H(\mathbf{c})|v^P(\mathbf{c})\rangle}{[E^P(\mathbf{c}) - E_j^Q(\mathbf{c})]^2} = \log \sum_j \frac{\langle v^P(\mathbf{c})|H(\mathbf{c})|v_j^Q(\mathbf{c})\rangle \langle v_j^Q(\mathbf{c})|H(\mathbf{c})|v^P(\mathbf{c})\rangle}{\langle v^P(\mathbf{c})|[H(\mathbf{c})]^2|v^P(\mathbf{c})\rangle} + A + B(\mathbf{c}), \quad (\text{S12})$$

where A is a constant and $B(\mathbf{c})$ averages to zero over the entire domain of \mathbf{c} . While the function $B(\mathbf{c})$ is unknown, it will be dominated by the large variations in the logarithm of the error as more and more training points are added. We note that

$$\begin{aligned} \sum_j \frac{\langle v^P(\mathbf{c})|H(\mathbf{c})|v_j^Q(\mathbf{c})\rangle \langle v_j^Q(\mathbf{c})|H(\mathbf{c})|v^P(\mathbf{c})\rangle}{\langle v^P(\mathbf{c})|[H(\mathbf{c})]^2|v^P(\mathbf{c})\rangle} &= \frac{\langle v^P(\mathbf{c})|H(\mathbf{c})(1-P)(1-P)H(\mathbf{c})|v^P(\mathbf{c})\rangle}{\langle v^P(\mathbf{c})|[H(\mathbf{c})]^2|v^P(\mathbf{c})\rangle} \\ &= \frac{\langle v^P(\mathbf{c})|[H(\mathbf{c}) - H^P(\mathbf{c})]^2|v^P(\mathbf{c})\rangle}{\langle v^P(\mathbf{c})|[H(\mathbf{c})]^2|v^P(\mathbf{c})\rangle} = \frac{\langle v^P(\mathbf{c})|[H(\mathbf{c}) - E^P(\mathbf{c})]^2|v^P(\mathbf{c})\rangle}{\langle v^P(\mathbf{c})|[H(\mathbf{c})]^2|v^P(\mathbf{c})\rangle}. \end{aligned} \quad (\text{S13})$$

We therefore arrive at the variance error estimate used in the main text,

$$\log\|v_{\perp}(\mathbf{c})\| = \frac{1}{2} \log \frac{\langle v^P(\mathbf{c})|[H(\mathbf{c}) - E^P(\mathbf{c})]^2|v^P(\mathbf{c})\rangle}{\langle v^P(\mathbf{c})|[H(\mathbf{c})]^2|v^P(\mathbf{c})\rangle} + A + B(\mathbf{c}). \quad (\text{S14})$$

Model 2 Hamiltonian

Model 2 describes four-distinguishable particles with equal masses m on a three-dimensional lattice with pairwise point interactions with coefficients c_{ij} for each pair $i < j$. We use lattice units where physical quantities are multiplied by powers of the spatial lattice spacing to make the combinations dimensionless. We take the common mass m to equal 1 in lattice units. We let \mathbf{n} denote the spatial lattice points on our three dimensional L^3 periodic lattice. Let the lattice annihilation and creation operators for particle i be written as $a_i(\mathbf{n})$ and $a_i^\dagger(\mathbf{n})$ respectively. The free non-relativistic lattice Hamiltonian has the form

$$H_{\text{free}} = \frac{3}{m} \sum_{i=1,2,3,4} \sum_{\mathbf{n}} a_i^\dagger(\mathbf{n}) a_i(\mathbf{n}) - \frac{1}{2m} \sum_{i=1,2,3,4} \sum_{\hat{\mathbf{1}}=\hat{\mathbf{1}},\hat{\mathbf{2}},\hat{\mathbf{3}}} \sum_{\mathbf{n}} a_i^\dagger(\mathbf{n}) \left[a_i(\mathbf{n} + \hat{\mathbf{1}}) + a_i(\mathbf{n} - \hat{\mathbf{1}}) \right]. \quad (\text{S15})$$

We add to the free Hamiltonian single-site contact interactions, and the resulting Hamiltonian then has the form

$$H = H_{\text{free}} + \sum_{i < j} \sum_{\mathbf{n}} c_{ij} \rho_i(\mathbf{n}) \rho_j(\mathbf{n}), \quad (\text{S16})$$

where $\rho_i(\mathbf{n})$ is the density operator for particle i ,

$$\rho_i(\mathbf{n}) = a_i^\dagger(\mathbf{n}) a_i(\mathbf{n}). \quad (\text{S17})$$